Transport in Porous Media **33:** 257–278, 1998.

Generation of Realistic Porous Media by Grains Sedimentation

MARCO PILOTTI
Dipartimento di Ingegneria Civile, Università degli Studi di Brescia, 38, Via Branze, 25123 Brescia, Italy. e-mail: pilotti@bsing.ing.unibs.it

(Received: 31 July 1997; in final form: 11 May 1998)

Abstract. In a recent paper, Tacher and co-workers proposed an interesting numerical technique to generate granular porous media. In this contribution, we present a similar procedure based on a sedimentation algorithm, that is able to overcome some of the difficulties present in the former technique. These are: (a) the impossibility to choose *a priori* a grading curve for the generated medium while retaining a realistic stacking where each grain is connected to at least three of its neighbours, and, (b) the random pattern of the grains in the porous medium, arising from their location inside the remaining void space of a box according to an arbitrary space filling criterion. We propose to generate three-dimensional granular media by simulating the deposition of spherical grains in a viscous fluid. We argue that the resulting chaotic grain pattern, by reflecting the actual generation process of sedimentary aggregates more closely, provides a better image of the complex topology of natural granular porous media. Although the generated medium is made up of spheres, it can be transformed, by changing the geometry of the grains through suitable domain mappings. The resulting three-dimensional porous media provide a realistic boundary for the numerical solution of linearized Navier–Stokes equations.

Key words: microscopic scale, intergranular void space, Stokes' flow, granular media.

1. Introduction

The slow viscous flow of a fluid in a saturated porous medium has been originally investigated by Darcy (1856), who experimentally derived the well known relation between the effective seepage velocity $\mathbf{v}$ [m/s], the dynamic viscosity coefficient μ [Pa s] and the macroscopic pressure gradient

$$\mathbf{v} = -\frac{k}{\mu}\nabla p, \tag{1}$$

through the introduction of the scalar permeability coefficient, k [m^2]. Relation (1), although modified with the introduction of the permeability tensor $\mathbf{K}$ in substitution of k, remains at the very heart of the theory of flow in porous media. In particular, the empirical nature of relation (1) has long been replaced by a theoretical derivation, through integration on a suitably large domain of the averaged, steady-state incompressible Stokes equations

$$\rho\mathbf{f} - \nabla p + \mu\Delta\mathbf{u} = 0, \qquad \nabla\cdot\mathbf{u} = 0, \tag{2}$$

where ρ [kg m^{-3}] is the mass density of the fluid, **u** [m s^{-1}] is the local velocity vector and **f** [m s^{-2}] the body force acting on the fluid per unit mass.

There is a wide consensus that the comprehension of the flow properties at the macroscopic scale (1) can benefit from the quantitative study of the interaction of the flow field at the micro scale (as represented by solutions of (2)) with the geometry of realistic porous media. This is apparent if one considers that important properties for the study of the averaged flow field in porous media have long been related to properties descriptive of the topology of void spaces. Just to mention a few, this is the case of the formation factor and of absolute permeability, that has been shown (e.g. Bear, 1988) to depend on porosity, tortuosity and an areal quantity related to the cross-section of the elementary channels through which the flow takes place. Here it is relevant to emphasise that nowadays it is computationally feasible to solve Equations (2) at the pore scale (see, e.g. Rothman, 1988; Chen *et al.*, 1991; Di Pietro *et al.*, 1994; Martys *et al.*, 1994; Maier *et al.*, 1998), in order to investigate the relation between microscopic properties and flow properties at the elementary volume scale. In this direction, as shown by Adler (1992) *inter alia*, a further important step lies in the generation of realistic porous media.

Structural properties of granular aggregates are a topic of considerable multi-disciplinary interest. Accordingly, over the last few decades many papers dealing with experimental (Dexter and Tanner, 1972; Wakeman, 1975; Onoda and Liniger, 1990; *inter alia*) and theoretical investigation (e.g. Torquato, 1987; Rubinstein and Torquato, 1989; Torquato and Lu, 1990; Torquato, 1992, 1994; Quintanilla and Torquato, 1996) of grain mixture properties have been published. More recently, a growing number of studies have taken advantage of the possibilities offered by synthetically reproduced porous media, that allow a thorough quantitative investigation of a medium topology. To this purpose, several generation techniques have been presented in literature, ranging from non-ballistic methodology (e.g. Jodrey and Tory, 1985; Martys *et al.*, 1994; Tacher *et al.*, 1997), to ballistic procedures capable of producing packings of nonspherical grains (Buchalter and Bradley, 1994; Coelho *et al.*, 1997). Ballistic algorithms usually simulate the sequential deposition of grains and operate both in a discrete or continuous space. They basically differ for the level of detail in the description of the interaction of the settling grain with the already settled particles (e.g. Jullien and Meakin, 1987). Actually, one of the stumbling blocks in the ballistic generation of porous media arises from the complexity of the interaction of the falling grain with potentially all the already settled grains. Accordingly, most of the ballistic simulations are limited to sphere distributions with a small variation coefficient of the diameter (typically, monodisperse or bidisperse distributions). With these grading curves, the falling grain does not penetrate the porous medium and stops after a limited interaction with the current upper layer.

In a recent paper, Tacher *et al.* (1997) have proposed an algorithm for generating three-dimensional random porous media. Following Allen (1985), this methodology is here defined as *random* in the sense that the grain packing is produced independently of a directed force. The idea at the basis of the method is that of

introducing grains into a control volume in a random fashion, starting from the coarsest diameter between an upper and a lower cut-off, until all spaces capable of holding a complete particle without overlapping have been used up. Accordingly, although quite simple, this procedure does not allow to control the final grading curve of the porous medium and requires the specification either of a minimum grain radius or a final porosity. Alternatively, if the grading curve is specified, the inserted grain is not necessarily connected to others anymore, so the resulting packing is a slightly realistic one. Although this methodology is quite interesting for its capability of producing complex three-dimensional structures, we share Adler's opinion (Adler, 1992) that pure chance is not sufficient to describe real porous media. This opinion can be easily substantiated if one considers, for example, that important properties of granular porous media depend on processes acting along preferential directions, such as deposition and compaction. In several cases these processes determine the anisotropy of the permeability tensor **K**.

In order to help overcome these difficulties, in this paper we present a methodology to generate granular porous aggregates by simulating the sedimentation of spherical grains in the limit of zero-inertia forces, as in a viscous fluid. This procedure is based on a sequential ballistic algorithm as used by Coelho *et al.* (1997). These authors have proposed a remarkable methodology to settle nonspherical grains that does not solve Newton's laws of motion. In their algorithm, a settling grain moves under the action of a combination of steepest descent and conjugate gradient methods. Each increment that contributes to lower the particle barycenter without causing penetration into other grains is allowed and each elementary displacement is uncorrelated to the previous one. The method is a parametric one because an adjustable coefficient is introduced to discriminate between translational or rotational degrees of freedom, when both would lead to a decrease of the particle elevation. Here we propose a nonparametric algorithm that simulates the settling process of spherical grains. We solve the law of motion for the falling grain, simulating the interaction with the already settled particles under the hypothesis of smooth constraints. Accordingly, the falling grain does not change its angular momentum. Although this could possibly lead to a higher packing density, the comparison of simulated media with some experimental results available in literature confirms the effectiveness of the proposed methodology.

The porous medium resulting from the presented procedure is characterised by a user-specified granulometric curve. Its porosity, as well as the overall topology of the intergranular void space, arises naturally as a consequence of the deposition process. After the porous medium has been generated, the constraint on the spherical shape of the particles can be removed by operating an off-line transformation on the generated grains.

2. The Generation Process

Let us consider granular media made up of settled spheres. Although several algorithms for the ballistic generation of bidimensional porous structures have been

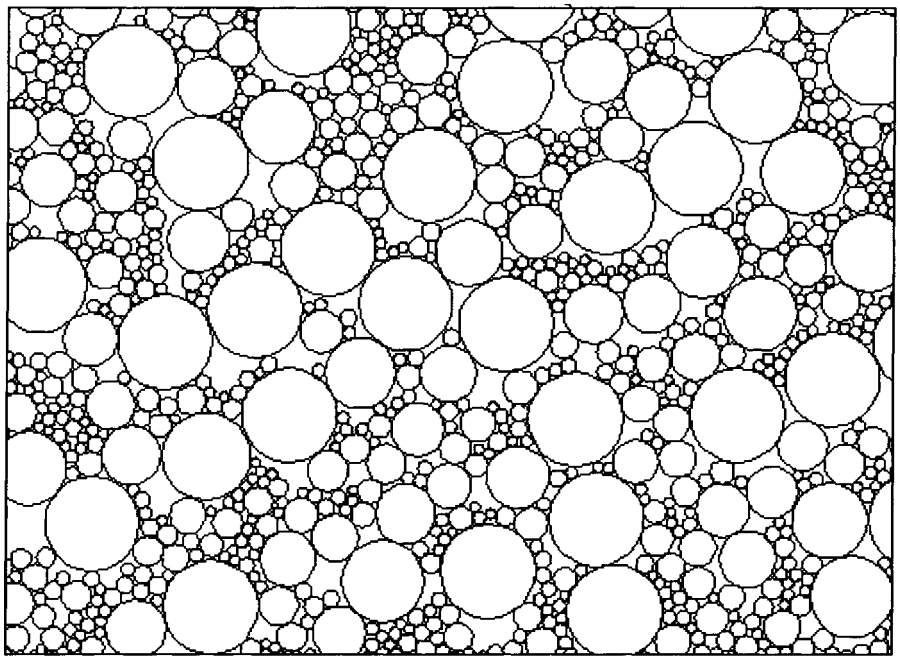

Figure 1. A two-dimensional porous medium, created by the deposition of randomly generated grains. This kind of porous medium can be regarded as an evolution of the traditional representation through bundles of straight capillary tubes, where flow is individually governed by Poiseuille flow. Accordingly, although interesting for several reasons (e.g. Ghilardi *et al.*, 1993), as far as the representation of the flow field is concerned it provides a deceptive visualisation of the complexity of real porous media. This can be easily realised if one considers that a medium like this is a strongly anisotropic one, where only the component k_{11} of permeability tensor **K** is different from zero, being 11 the index that refers to the direction orthogonal to the page. This figure can be compared with its three-dimensional counterpart in Figure 3(c).

proposed in literature (e.g. Ghilardi *et al.*, 1991, 1993; Jiang and Haff, 1993; Haff and Anderson, 1993; Jiang, 1995), when the grain arrangement is not trivial the passage to a three-dimensional one is not straightforward. The ballistic generation of a bidimensional porous medium (that can geometrically be seen as the orthogonal cross-section of a multiply connected cylinder), is rather simple and can be efficiently done by considering the interaction of a randomly generated falling grain with the upper layer of the deposed grains only. As a matter of fact, the falling grain cannot pass through the upper layer of the deposed medium, as this is (quite unrealistically) impervious in the vertical direction (see, e.g. Figure 1, where grains are circles). Accordingly, the grain, after a finite sequence of rotations and downward translations, settles when it rests in a stable position between two other grains of the upper layer. After this step, the upper layer is updated and the sedimentation process starts again. Adding one dimension greatly adds to the complexity of the problem, both from the point of view of the settling mechanics and information retrieval. On the other

hand, in our opinion it incomparably enhances the representativeness of the generated porous medium.

The general idea behind our algorithm for the generation of a three dimensional porous medium can be formulated as follows. A subspace in R^3 is selected where deposition will occur. Let us think of it as a box where spheres with an assigned diameter probability distribution are deposed in a fluid at rest, by initially inserting them at a random location $(x, y, z_{\max})$ on the upper part of the box. From this point the generated sphere starts falling, until it touches the bottom or another sphere that has been previously deposed.

Even from this simple preliminary description, the need for two basic ingredients is already evident. As a prerequisite, an algorithm for the efficient search of points located in a subspace of R^3 is required. Then, the deposition process must be modelled, retaining only the aspects of the grain settling mechanics that are deemed to be significant from the point of view of the final granular structure.

To appreciate the importance of the first point, it is sufficient to consider that in a three-dimensional ballistically generated porous medium, a falling grain does not interact only with the upper layer, but, at least potentially, with all the other grains that have been already deposed. Actually, when the grain linear dimension is sufficiently small with respect to that of the pores, it can penetrate through the porous medium as far as the bottom of the deposition box. On the other hand, it can be easily reckoned that, in order to obtain a realistic porous medium, where edge effects have been filtered out, sufficiently low d/L ratio must be kept, where d is the characteristic linear dimension of the grain and L is the length of the side of the deposition box. According to Ridgway and Tarbuck (1966), the effect of the hypothetical box walls in reducing the particle concentration (i.e. increasing the porosity) persists inwards over a distance of about five sphere diameters for uniform distributions. In the procedure proposed by Tacher *et al.* (1997), this type of effect is not present because of the unnatural way used to fill the control volume. Accordingly, a typical value of the aforementioned ratio is at least 50, so that one can easily realise that several dozens of thousands of grains must be deposed to generate a single realization of a three-dimensional porous medium. Given that during the deposition of a grain its position must be continuously checked with respect to that of grains already deposed, this clearly prompts the need for efficient algorithms with an optimal operation count to search for the spatial proximity of any given point in the box.

To this purpose an *octree* algorithm (see, e.g. Meagher, 1980; Yerry and Shephard, 1984) has been selected. This type of algorithm is an excellent $O(\log_8(N))$ algorithm devised for searching for points having an arbitrary spatial distribution, N being the dimension of the list to be searched. For simplicity's sake, the ideas behind the algorithm can be explained by making reference to the two-dimensional version of the method, known as *quadtree*.

In a quadtree algorithm the points of list P, where $P \subset R = [a, b] \times [c, d]$ (see Figure 2(a)) are sequentially introduced in a dynamically allocated, space-ordered structure. From a geometric point of view, the algorithm divides R in a cascade of

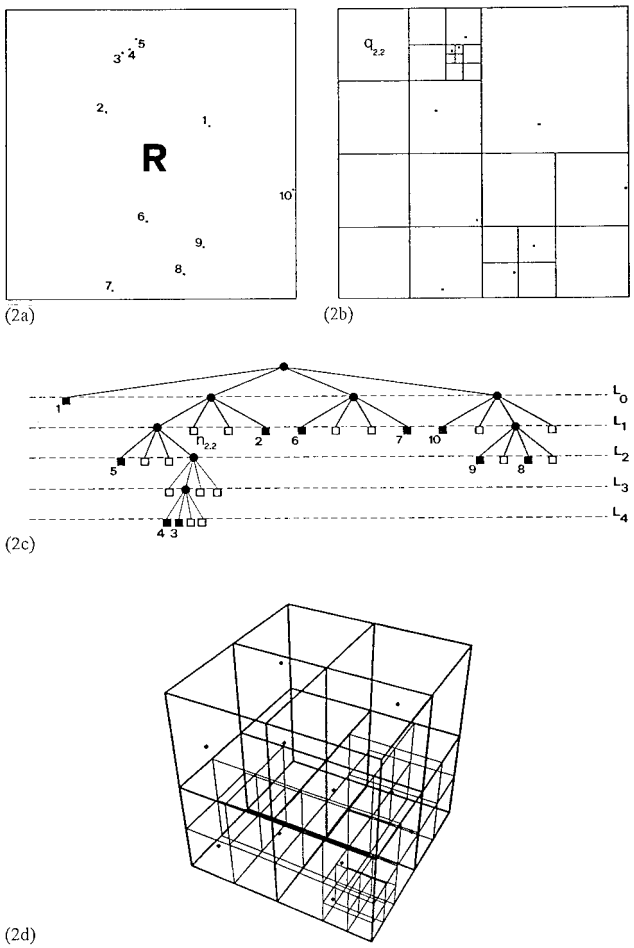

Figure 2. Logical organisation of set $P \subseteq R$ inside a quadtree structure. In Figures 2(a) and 2(b) the R space and the points p_i of list P are shown, along with the partition of R operated by the algorithm. In Figure 2(c) the tree structure corresponding to Figure 2(b) is shown. In Figure (2d) the partition of space operated by the octree algorithm is shown. Black dots represent the centres of already settled spheres in the tree-like structure at an intermediate stage of the generation of a porous medium.

quadrants (Figure 2(b)), whose level of nesting depends on the number and location of the points contained in *P.* This cascade can be efficiently represented by a tree-like structure, as shown in Figure 2(c) with reference to the set of points of Figures 2(a) and 2(b). Each node n_i of the tree represents a quadrant q_i in R. Three different conditions are possible for a node. It can be empty (represented by empty squares in Figure 2(c); e.g. node n_{2_2}, corresponding to the quadrant q_{2_2} in Figure 2(b)) when no point of P is contained inside q_i. Otherwise, it contains either a point $\mathbf{x}_i \in P$ (solid squares in Figure 2(c)) or four links to the four sub-quadrants directly nested in q_i (solid circles in Figure 2(c)). The latter situation happens when, during the sequential

introduction of a point in the tree (e.g. $\mathbf{x}_{i+1}$), the point falls inside a quadrant at level L_j where another point (e.g. $\mathbf{x}_i$) is already present. In such a case, the quadrant is subdivided into four and the old point $\mathbf{x}_i$ is moved into its respective quadrant at level L_{j+1}. Then point $\mathbf{x}_{i+1}$ is introduced to the new quadrant into which it falls. If this quadrant is full again, the subdivision process is iterated until a quadrant with vacant storage space is found. Accordingly, the information associated with the P points is contained only in the terminal nodes (*leaves*) of the tree.

During the search, the tree is explored and R is optimally partitioned, simply by checking the co-ordinates of the quadrant corresponding to the current tree node. For example, when the problem is that of finding the points that lie inside a given region, we go down the levels of the quadtree, eliminating at the highest possible level the quadrants that lie outside the search region.

Let us now consider the dynamics of the falling grain. As a preliminary observation, it should be noted that our purpose is not that of reproducing the dynamics of a settling grain as much as that of building a granular structure similar to that turning out from a sedimentation process in a viscous fluid at rest, where accelerations are negligible and a small asymptotic falling speed is rapidly attained. Accordingly, we shall assume that the grain is a rigid body characterized only by three translational degrees of freedom, the three rotational degrees of freedom being irrelevant to our analysis. Two events may stop the downward motion of a settling grain. The first is when the grain gets to the bottom of the box. The second happens when the grain attains a stable position between the mass centres of three other grains. In both cases the centre of the new grain is inserted in the proper position inside the octree structure and the generation process is iterated again. Generally, both these events are preceded by the interactions with the surface defined by grains already settled. Here, in order to reduce the level of complexity, another assumption has been made. We basically assumed (as implied by the small settling velocity) that the momentum transfer between the falling grain and the ones already settled is negligible. Accordingly, a resting grain cannot be dislodged from its position as a consequence of the interaction with a falling one. In the same way, the collisions do not cause the falling grain to bounce. When a grain comes into contact with another grain, it sticks to its surface and it moves under the action of its weight and of the constraining reaction exerted by the surface. The dynamics of a sphere having radius R, moving on a surface made up by other spheres $(r_i, \mathbf{x}_i)$, where r_i is the radius and $\mathbf{x}_i$ the vector-like representation of the centre of the ith sphere, is in our case equivalent to the sliding motion of a point (i.e. the centre of the falling sphere) on a second surface, $\psi(x, y, z)$. This surface is given by the envelope of spheres $(r_i + R, \mathbf{x}_i)$ and, accordingly, is piecewise defined as

$$(\mathbf{x} - \mathbf{x}_i)^2 = (R + r_i)^2. \tag{3}$$

The dynamics of a point p moving on a surface $\psi(x, y, z)$ can be modelled by the equation

$$m\mathbf{a} = \mathbf{F} + \lambda(p)\nabla\psi, \tag{4}$$

where **F** [N] is the external force acting on the point (in our case, the grain submerged weight) and $\lambda(p)\nabla\psi$ [N] is the constraining reaction exerted on p, under the hypothesis of smooth constraints. Equation (4) corresponds to a system of three scalar equations from which $\lambda(p)$ can be eliminated, obtaining the two differential equations

$$\begin{aligned} ma_y &= F_y + \frac{ma_x - F_x}{\partial\psi/\partial x}\,\frac{\partial\psi}{\partial y}, \\ ma_z &= F_z + \frac{ma_x - F_x}{\partial\psi/\partial x}\,\frac{\partial\psi}{\partial z}, \end{aligned} \tag{5}$$

that coupled to the locally known Equation (3) provide the laws of motion $x(t)$, $y(t)$ and $z(t)$ of the grain centre. From these the trajectory of the point and the proportionality coefficient $\lambda(p)$ of the constraining reaction can be computed. In particular, if the constraint is unilateral, when $\lambda(p) = 0$ the point abandons the surface and continues its free fall until a new contact with $\psi(x, y, z)$ is found.

If the inertia of the grain is small, as supposed so far, the grain will come to rest when its centre will be located, in a stable configuration, between the mass centres of three other grains in the already settled porous medium. These three supports completely constraint the three translational degrees of freedom of the grain.

Special attention should be given to the situations in which $\nabla\psi$ is not defined on $\psi(x, y, z)$. This happens along the lines Γ_i and at the singular points $\hat{\mathbf{x}}_i$ on $\psi(x, y, z)$ that correspond to double and triple contacts between the falling grain and the ones already settled. In the former case, the motion of the falling grain is simulated as a rotation around the axis joining the centres of the two spheres that define the intersection Γ_i. In the latter, a check is performed to verify whether the attained configuration $\hat{\mathbf{x}}_i$ is a stable one for the falling grain. If the answer is negative, given that $\hat{\mathbf{x}}_i$ is the confluence of three Γ_i lines, the falling grain continues its downward motion along the direction that maximises the positive work of the grain weight.

So far we have considered grains of spherical shape. This is a very convenient way of representing the porous medium, since at the end of the generation process this is analytically fully described by the set $(\mathbf{r}_i, \mathbf{x}_i)$. Apart from the noticeable but particular case of oolite sandstone, made up of almost perfectly spherical particles, in our opinion, this type of conceptualisation can be easily extended to provide a good approximation for a rather wide class of porous media, deriving from the deposition of water worn sediments. As a first step, since a prolate spheroid is merely a stretched sphere, simply by operating the co-ordinate change

$$\begin{aligned} X &= nx, \\ Y &= my, \\ Z &= pz, \end{aligned} \tag{6}$$

that maps (x, y, z) into (X, Y, Z), it is possible to transform the settled spheres into elliptical grains in the (X, Y, Z) space, having the same orientation and honouring

the tangency condition that derives from the aforementioned settling mechanics. The porous medium turning out from transformation (6) is one characterised by a pre-defined anisotropy.

A more general mapping can be easily performed if one accepts that the granular medium can be made up of partly overlapping grains. As far as the geometry of the intergranular void space is concerned, the final effect induced by partial grain overlapping is similar to that caused by diagenetic processes such as cementation or pressure solution that can join several grains in a single larger one. For simplicity's sake, let us consider spherical co-ordinates r, φ, θ and let $S(\varphi, \theta)$ be the adimensional radial co-ordinate of an arbitrary shaped single-valued closed surface. Under such an unrestrictive hypothesis, that ensures that the surface does not lap over itself, a sphere of radius r_0 in (r, φ, θ) can be mapped in the arbitrary surface $\bar{r} = r_0 S(\bar{\varphi}, \bar{\vartheta})$ in $(\bar{r}, \bar{\varphi}, \bar{\vartheta})$ simply as

$$\begin{aligned} \bar{r} &= r\,S(\varphi, \vartheta), \\ \bar{\varphi} &= \varphi, \\ \bar{\vartheta} &= \vartheta. \end{aligned} \tag{7}$$

Accordingly, starting from the original $(r_i, \mathbf{x}_i)$ set, it is possible to obtain the void space delimited by the grains by subtracting to the deposition box a set of (possibly) overlapping grains shaped as $S(\varphi, \theta)$. In this case, an analytic definition of the porous medium becomes cumbersome. However, it is here relevant to observe that, as far as the numerical simulation of system (2) is concerned, an analytical definition of the boundary of the porous medium is not strictly necessary and can be effectively substituted by the void distribution function

$$\alpha(x) = \begin{cases} 1 & \text{if } x \text{ is inside the pores,} \\ 0 & \text{otherwise,} \end{cases} \tag{8}$$

that can be obtained by resampling the boundary description at discrete lattice sites. This happens, for instance, in the case of the simulations of flow in porous media performed by using lattice gas or lattice Boltzmann techniques (e.g. Rothman, 1988; Di Pietro *et al.*, 1994; Pilotti and Menduni, 1997; Maier *et al.*, 1998), where the boundary conditions along the solid boundary are easily implemented on the basis of the Boolean state of function (8). In Figure 10(b) we provide an example of a cross-section of a porous medium generated according to distribution C of Table I and mapped by using a simple trigonometric transformation

$$\bar{r} = r \left[1 + \sum_{j=1}^{3} \left(C_j \cos(\omega_j \vartheta)^a \sin(\omega_j \vartheta) \right) \right] \cdot \left(\frac{\pi}{2} - abs(\varphi) \right),$$

$$0 \leqslant \vartheta \leqslant 2\pi, \quad -\frac{\pi}{2} \leqslant \varphi \leqslant \frac{\pi}{2},$$

where the parameters C_j, ω_j and a have been appropriately changed from grain to grain. This distribution, for a suitable choice of the parameters, does not change the

Table I. Cumulative probability distributions $F(r)$ as a function of sphere radius r along with the observed porosity ϕ and specific surface S, for the 6 mixtures studied by Dexter and Tanner (1972) and numerically investigated in this paper. Mixture A corresponds to a monodisperse distribution.

r [m]	$F(r)$					
	A	B	C	D	E	F
0.001191	0	0.000959	0.065296	0.219066	0.339179	0.413466
0.001588	0	0.030501	0.249372	0.474406	0.601903	0.669966
0.001984	0	0.139416	0.423726	0.624666	0.72598	0.777425
0.002183	0	0.239562	0.528804	0.702848	0.786238	0.827723
0.002381	0	0.415222	0.665186	0.794056	0.853218	0.88214
0.002778	0	0.658711	0.799686	0.873947	0.908693	0.925899
0.003175	1	0.827394	0.884531	0.92271	0.942064	0.952006
0.003572	1	0.958998	0.955766	0.964668	0.971126	0.974907
0.004366	1	0.987505	0.980189	0.981555	0.983727	0.985229
0.004763	1	0.994549	0.9886	0.988065	0.988878	0.989559
0.005159	1	0.999473	0.996998	0.995534	0.995103	0.995001
0.00635	1	1	0.999823	0.999442	0.999132	0.99894
0.008731	1	1	1	1	1	1
ϕ [-]	0.406	0.402	0.3806	0.3727	0.3675	0.3584
S [m^{-1}]	561.3	581.98	621.2	650.94	674.44	697.14

average radius of the spherical grain on which it operates. More realistic transformations can easily be devised on the basis of the quantitative analysis of the geometry of grain particles (e.g. Heywood, 1937).

A concluding consideration regards the computational burden of the algorithm – although not straightforward, the presented procedure is sufficiently fast to allow implementation on a microcomputer. To be generated, all the cases presented in this contribution require a few hours of simulation on a 486 DX4 PC.

3. The Geometry of the Resulting Porous Medium

Jullien and Meakin (1987) have studied several three-dimensional off-lattice models for ballistic deposition of monodisperse particles, each characterised by increasing level of detail in the description of the interaction between the settling grain and the upper layer of the deposit. The strong porosity variation of the resulting porous media (between 0.853 and 0.418) computed by these authors, suggests both the importance of using a physically based approach to the generation of synthetic granular porous media and the importance of comparing numerical results with experimental measurements obtained by mixtures of spheres settled in similar conditions. Since

it has been observed that granular materials even with the same distribution do not pack to a unique porosity (e.g. Gray, 1968), in the following, due to the absence of a compaction process in our simulations, the comparison will be referred to loose packings.

Having a mathematical description of the porous medium, a thorough investigation of its topology is possible. As an example, here we shall consider some of the parameters that are typically used to characterise grain packings, *viz.* porosity ϕ [-], specific surface S [m^{-1}] and the coordination number C [-]. While porosity and specific surface (i.e. the overall interstitial surface area of the pores per total volume of the sample) are closely related to the medium permeability, the coordination number (i.e. the average number of grains with which each particle is in contact) provides an example of an important structural parameter that cannot be easily measured from an experimental point of view. The analysis will be limited to porous media obtained by deposition of grains having uniform, fractal and lognormal distributions. Whereas the uniform distribution corresponds to the simplest possible mixture of grains, the fractal probability distribution

$$P(\xi < r) = \begin{cases} P(\xi < r) = 0 & r < r_{\min} \\ \dfrac{1 - (r/r_{\min})^{-n}}{1 - (R_{\max}/r_{\min})^{-n}} & r_{\min} \geqslant r \geqslant R_{\max} \\ P(\xi < r) = 1 & r > R_{\max}, \end{cases} \tag{9}$$

(where n is the fractal dimension and $r_{\min}$ and $R_{\max}$ are the lower and upper cut-offs of the fractal medium) has been proposed by Turcotte (1986, 1992) for sediment mixtures deriving from a fragmentation process. The rationale behind using (9) is that, with the exception of particles finer than silt, the origin of sediment is often fragmentation. In reality, although the genesis of the fragments might be governed by (9), sediment transport and deposition is usually size selective so that the actual granulometric curve may differ (and often does) from a fractal curve. In particular, the lognormal distribution is an interesting approximation of the grading curve for the grains of several sedimentary rocks, as it has been shown (Spencer, 1963; Vischer, 1969; Garde, 1972; Kothiari, 1995) that natural size distribution curves are essentially mixtures of three or less fundamental populations of lognormal grain sizes.

Figure 3(b) shows a plug obtained by deposition of grains having uniform distribution, where only the intergranular void space has been retained, to provide a qualitative idea of the boundaries of the flow fields. As shown in Figure 3(a), this plug has been extracted from a core that corresponds to the deposition control volume, built sufficiently larger in order to avoid the mentioned wall effects. As shown in Table II (mixture *A*), the computed porosity for uniform samples like that in Figure 3(b) is around 0.418, a value that compares favourably with several results available in the literature. In the same experimental conditions, Dexter and Tanner (1972) have measured a porosity value of 0.406. Onoda and Liniger (1990) have studied the onset of dilatancy on a mixture of mono-distributed glass spheres settled in a

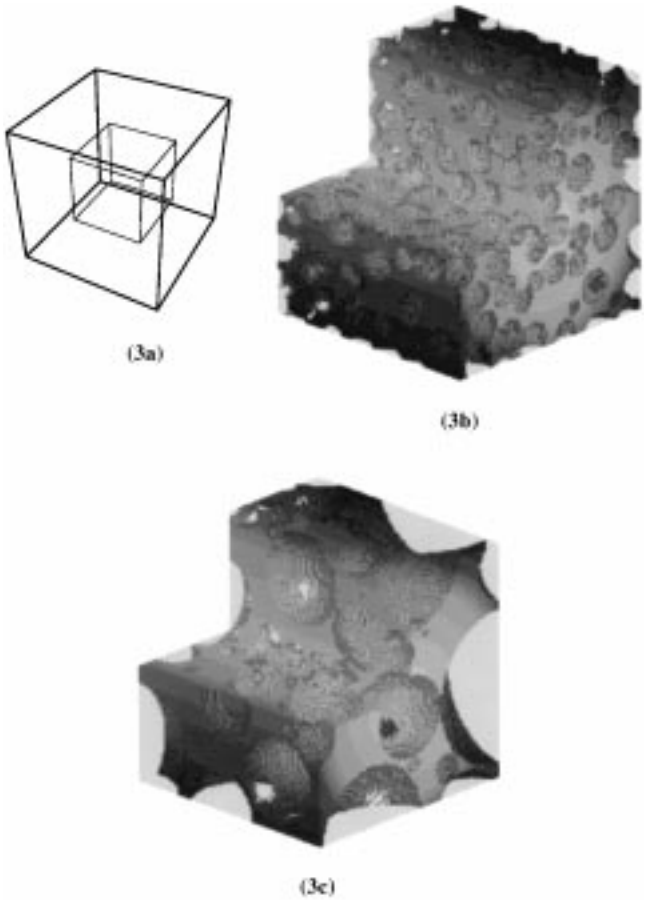

Figure 3. The deposition box (3(a), in bold) and the profile of the cylindrical core (inner box) used for the extraction of the wall-undisturbed samples (plugs) shown in 3(b) and 3(c). In these figures the intergranular void space inside the generated granular porous media is shown. The figures correspond to two different granulometric curves, each characterised by the same ratio $L/R_{50} \simeq 90$, being L the side of the deposition box and R_{50} the average radius of the deposed mixture. The case shown in 3(b) corresponds to a uniform grain distribution, whereas 3(c) corresponds to the fractal distribution (9), with $n = 1.6$ and $R_{\max}/r_{\min} = 10$. This is the three dimensional counterpart of the porous medium shown in Figure 1.

liquid. In order to control the effect of gravity on the packing density up to the limit of a neutrally buoyant condition, they have studied the variation of porosity with the density of the liquid, measuring a variation between 0.403 and 0.445. The latter value has been obtained at the limit of zero submerged weight of the glass spheres used in the experiments. A porosity value of 0.4 is supported also by the experimental findings of Berryman (1983) for a monodisperse mixture in loose conditions. Coehlo *et al.* (1997) in their numerical experiments have computed a porosity of 0.4121 while the fourth model proposed by Jullien and Meakin (1987) provides a value of 0.418.

Table II. Porosity (ϕ), specific surface (S), coordination number (C) and maximum number of contacts (M) computed for the samples generated according to the distributions of Table I.

	$F(r)$					
	A	*B*	*C*	*D*	*E*	*F*
ϕ [-]	0.418	0.404	0.392	0.379	0.371	0.365
S [m^{-1}]	550.2	583.7	621.3	656.1	689.5	701.9
C [-]	6.43	6.62	6.72	6.72	6.73	6.73
M [-]	10	19	37	54	64	70

A systematic analysis has been performed on lognormally distributed packings, using the experimental results provided by Dexter and Tanner (1972) who have studied mixtures of spheres obtained by mixing up to thirteen different size diameters to generate loose packings according to five lognormal distributions (mixtures B, C, D, E, F), whose cumulative curves are shown in Table I. The authors have measured the density of samples generated by carefully pouring a pre-mixed distribution into cylindrical containers having a circular cross-section. For each mixture the whole process was repeated four times, observing a variation of less than 1% in the measured results, whose average values are shown at the bottom of Table I.

In order to test the procedure presented in this paper, we have numerically repeated Dexter and Tanner's experiments by settling spheres corresponding to the distributions of Table I into cylinders of rectangular cross-section (see Figure 3(a)), whose dimensions have been chosen so that they are circumscribed about Dexter and Tanner's containers. The results of our simulations, repeated and averaged on four different realizations, are shown in Table II and in Figures 4(a)–4(d). In Figure 5 some vertical cross-sections of the plugs are shown while in Figure 6(a) vertical cross-section and a horizontal one are compared with reference to mixture *F*.

In Figure 4(a) we compare experimental and numerical porosity. As can be observed, our method overestimates porosity no more than 3%. However, it should be taken into account that our simulations have been performed by settling spheres in a rectangular vessel, where one can expect that the wall effect is higher than when using Dexter and Tanner's circular cylinders. Another information that can be computed from the original data provided by Dexter and Tanner regards the specific surface *S*, that is compared to the one of the simulated samples in Figure 4(b). In Figure 4(c) we show the computed coordination number. This is an information that cannot be derived from Dexter and Tanner's data and that is rather difficult to measure from an experimental point of view. Our numerical results show that in this case the coordination number does not significantly increase for samples *C, D, E* and *F*. What increases (see Figure 4(d)) is the maximum number of contacts observed inside the samples, that seems to be linearly related to porosity.

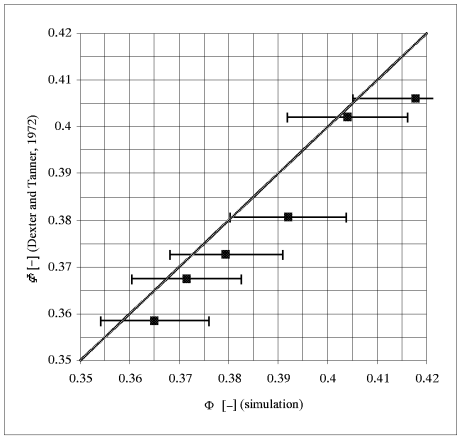

(4a)

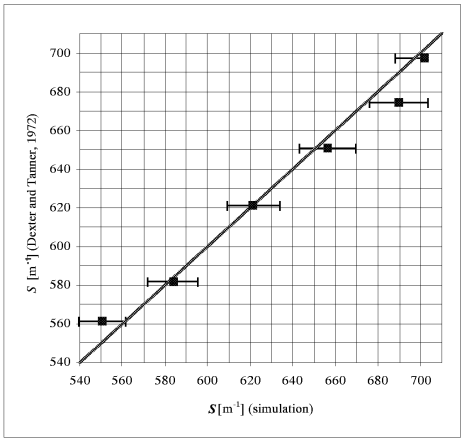

(4b)

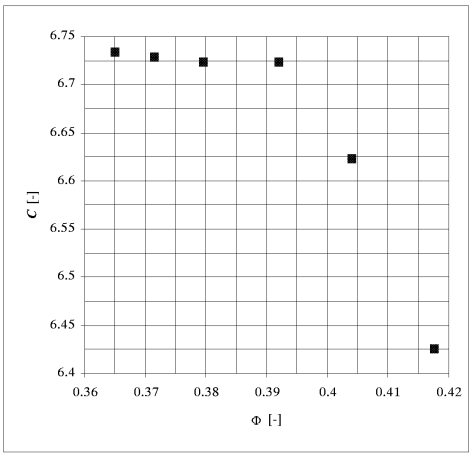

(4c)

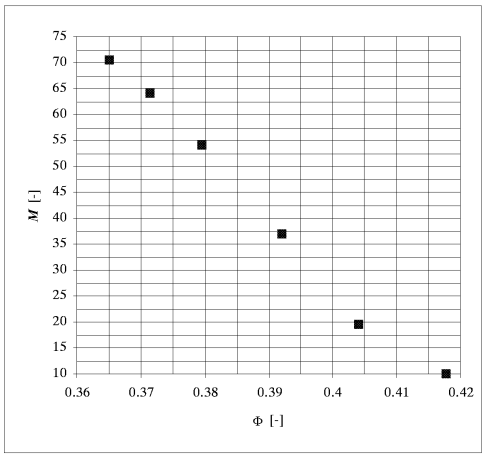

(4d)

Figure 4. In Figures 4(a) and 4(b) the comparison between measured and computed porosity (ϕ) and specific surface (S) are shown. The error bars correspond to a 3% limit. Figures 4(c) and 4(d) show the computed coordination number and the maximum number of contacts for a single grain, as a function of the computed porosity.

The same measurements have been performed on samples generated according to distribution (9), where n has been varied between 0.5 and 3, and the $R_{\max}/r_{\min}$ ratio has been kept equal to 10. The results are shown in Table III, while typical vertical and horizontal cross-sections are shown in Figure 7. It may be interesting to note that if one keeps $R_{\max}/r_{\min}$ constant, increasing n does not lead to a decrease of ϕ, while in the case of the lognormal distributions investigated by Dexter and Tanner the porosity is negatively correlated to the mixture standard deviation. Although no counterpart of Dexter and Tanner's experiments for distribution (9) is available to our knowledge, the computed porosity value for $n = 1.5$ (Figure 7(i)) can be

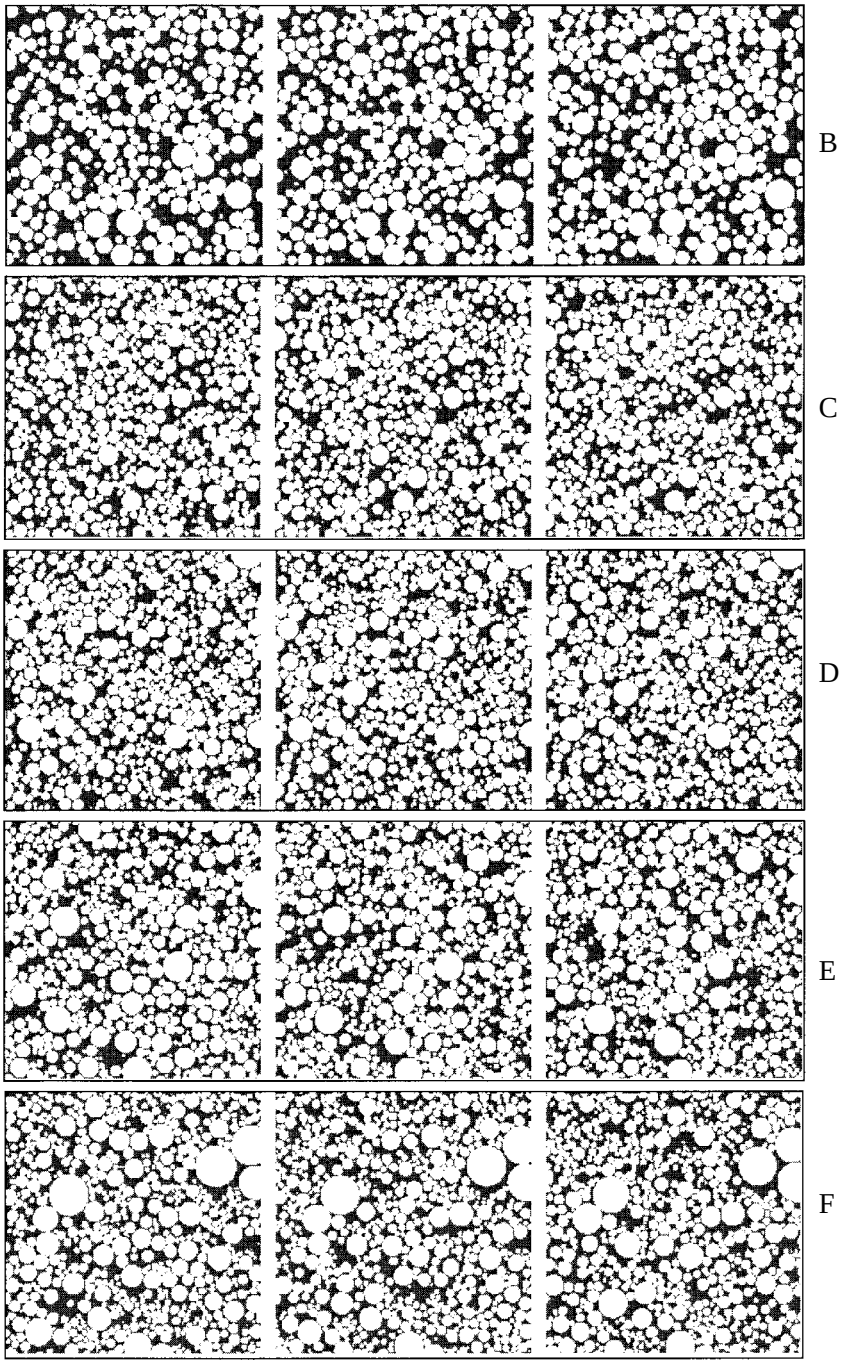

Figure 5. Vertical cross-sections obtained by samples generated according to the lognormally distributed mixtures investigated by Dexter and Tanner (1972). Letters refer to Table I.

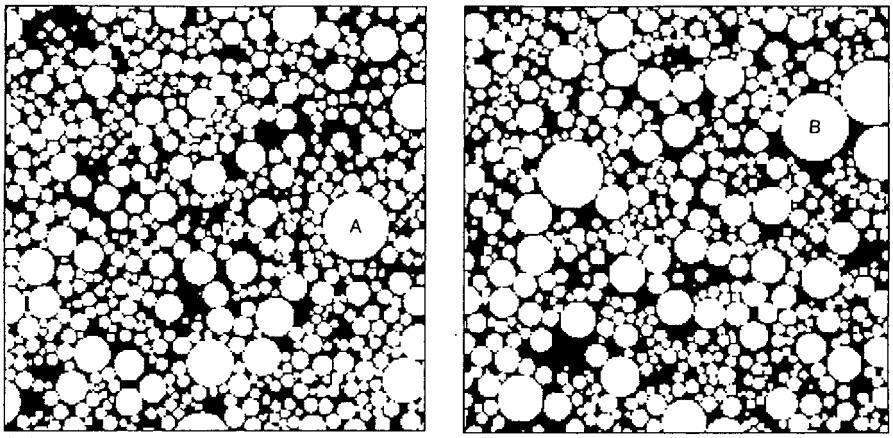

Figure 6. Comparison between a horizontal cross-section (a) and a vertical one (b) corresponding to mixture *F* of Table I. In the vertical cross-sections, the poorer the grain sorting, the more evident the sheltering effect of larger deposed grains is, deriving from the ballistic nature of the genetic algorithm. This can be observed if one compares, for example, the situation around grain *B* with the grains arrangement around grain *A*.

Table III. Porosity (ϕ), specific surface (S), coordination number (C) and maximum number of contacts (M) numerically computed for 6 samples generated according to distribution (9) ($R_{\max}/r_{\min} = 10$).

	$F(r)$					
	$n = 0.5$	1	1.5	2	2.5	3
ϕ[-]	0.364	0.358	0.332	0.324	0.33	0.355
S [m^{-1}]	3145	3641.7	4529	5488.2	6971.3	8067
C [-]	6.19	6.33	5.55	5.71	5.86	5.93
M [-]	36	44	59	77	96	130

compared to a result experimentally observed by DallaGiovanna and Vitali (1996), who have measured the properties of granular aggregates obtained by sedimentation of rounded grains, mixed according to distribution (9). These authors, working on several samples, have measured a volumetric porosity ranging between 0.27 and 0.3. In our opinion, these lower porosity values can be explained both due to a natural compaction process, that is not taken into account in the presented algorithm, and due to the considerably wider range of the linear dimension of the deposed sediment. Actually, while DallaGiovanna and Vitali have worked with mixtures characterised by a $R_{\max}/r_{\min}$ ratio of approximately 100, due to memory constraints we limited our simulation to the range $R_{\max}/r_{\min} = 10$.

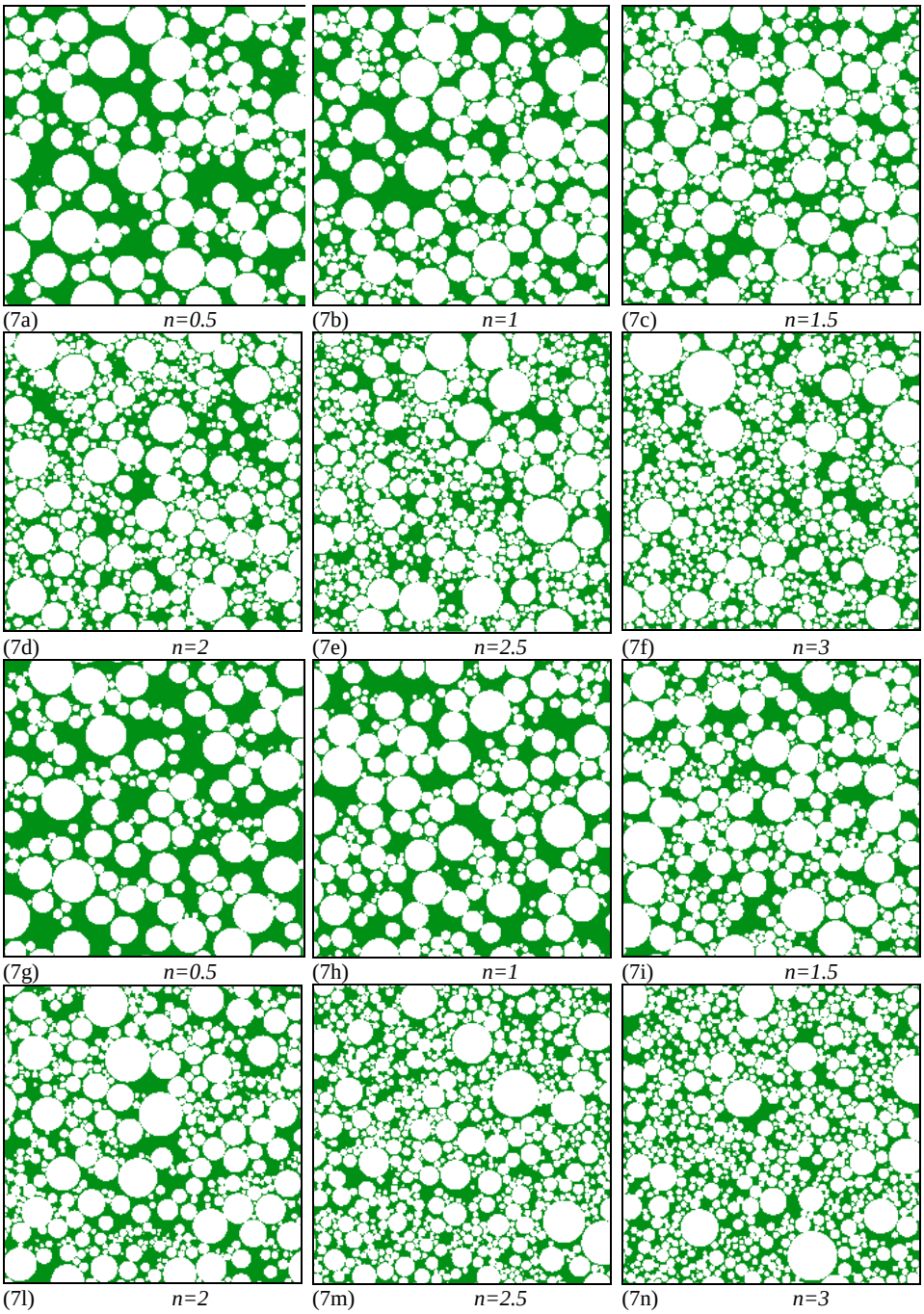

Figure 7. Horizontal (a–f) and vertical (g–n) cross-sections for porous media obtained according to distribution (9) ($R_{\max}/r_{\min} = 10$).

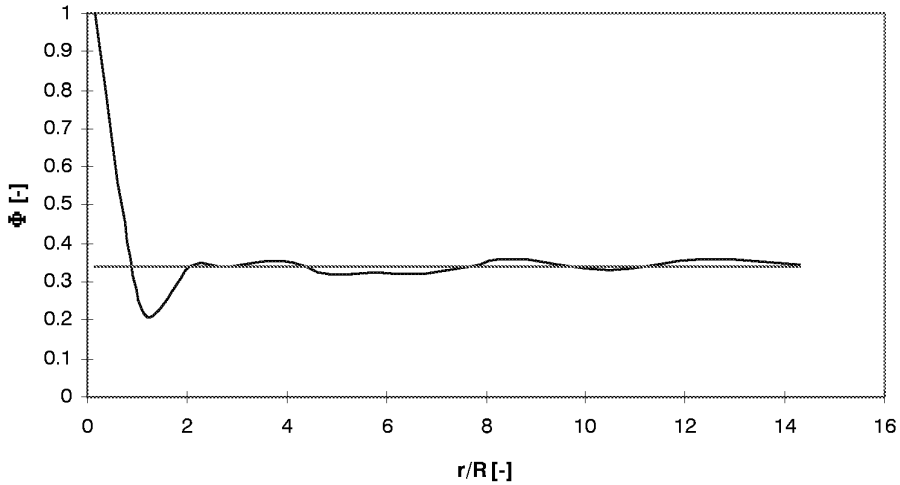

Figure 8. Porosity for the sample shown in Figure 3(c), as a function of the radial distance from the physical centre (x_c, y_c, z_c) of the control volume. This is an example of identification of the representative elementary volume (REV) associated with volumetric porosity $\phi(x_c, y_c, z_c)$. Distance r from (x_c, y_c, z_c) is normalised with the average radius R_{50}.

It may be interesting to compare Figure 7(i) with Figure 1, approximately reflecting the same grain distribution. As could be expected, the three-dimensional porous medium is not impervious in the x and y horizontal directions and presents a different void space dynamic. If we define the horizontal area of a cross-section as A and the overall area occupied by grains in the same cross-section as B, the observed areal porosity is the complementary set $C = A - B$. In a three-dimensional porous medium generated by sedimentation, grains are deposed on different horizontal planes. Accordingly, the B set is the union of grain areas obtained by sectioning the spheres along generic horizontal planes, whilst B in Figure 1 is obtained by equatorial sections of a statistically equivalent spheres set. Accordingly, in the latter case B is maximised and, in turn, the porosity is minimised. This obviously questions the validity of some conclusions derived by reasoning on simplified two-dimensional structures like that portrayed in Figure 1.

The volumetric porosity associated with the fractally distributed sample of Figure 3(c) has been investigated in Figure 8, where the porosity continuum scale (REV, Bachmat and Bear, 1986) has been identified. As can be observed, as far as porosity is concerned, a continuum approach seems already possible as r is greater than $3R_{50}$, r being the radial distance from the centre (x_c, y_c, z_c) of the plug and R_{50} the average diameter of the grain size distribution curve.

As a concluding remark, a further example of the possibilities offered by our generation technique is that of providing a direct method for approximating the tortuosity of a streamline (see, e.g. Bear, 1988) passing through a generated porous medium. Quite simply, the trajectory of a fluid particle can be approximated by keeping track of the path followed by a test sphere (that must be tiny with respect

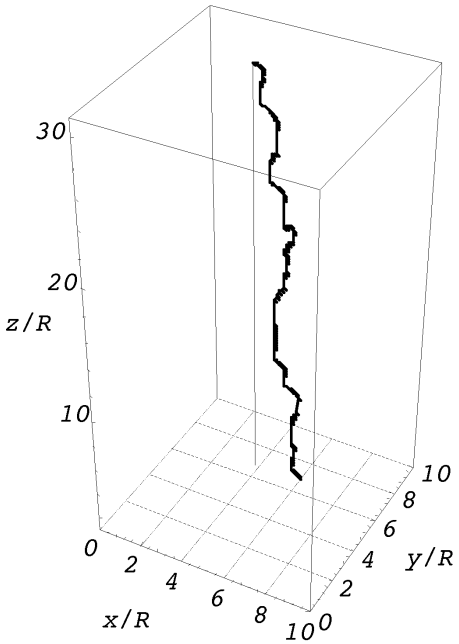

Figure 9. Tentative flow trajectory (line in bold) of a material point crossing the core corresponding to Figure 3(b) under the action of a vertical driving force, compared with a straight line starting from the same entry point (distances are normalized with the average radius R_{50}). The computed tortuosity value is 0.89.

to the characteristic linear dimension of the intergranular void space), falling inside the void space of a generated porous medium. Due to its dimension, the sphere is not intercepted during its fall and it contours the deposed grains, until the bottom of the sample is reached. An example is given in Figure 9, where a trajectory is shown with reference to the sample shown in Figure 3(b). The measured tortuosity value, in the considered direction is approximately 0.89. Needless to say, this procedure, approximating the motion of a particle under the action of a vector (the gravity acceleration) that is constant in space, provides only a tentative trajectory for a fluid particle, whose real motion is governed by the space varying pressure field and whose exact determination requires the solution of Equations (2).

4. Conclusions

This paper is the preliminary part of a research project currently under way on the solution of Stokes equations in three-dimensional granular porous media. We believe that the physical comprehension of flow in porous media can benefit from a better understanding of the physics of flow at the microscale. In this direction, an important prerequisite is the identification of a procedure to reproduce the boundary that confines the flow field. This paper presents the outlines of an algorithm to

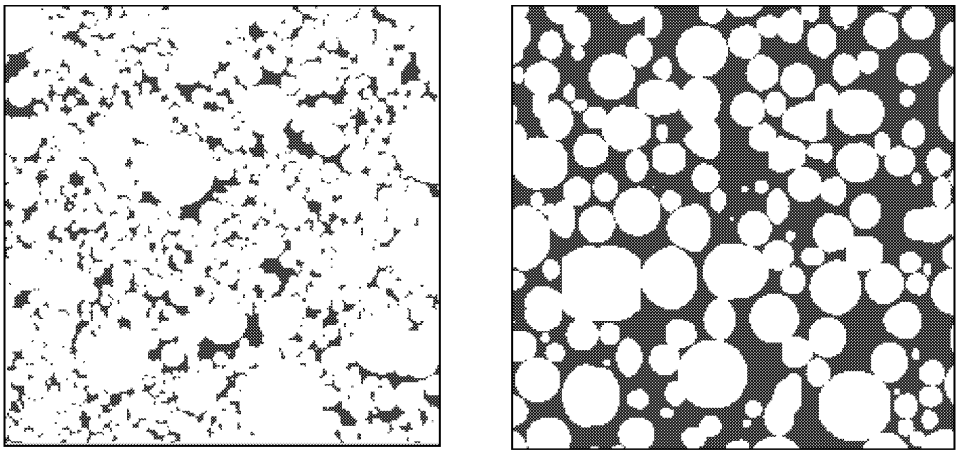

(10a) (10b)

Figure 10. The geometry of the resulting porous medium can be changed if one relaxes the tangency conditions between the grains. In this direction, grain indentation by pressure solution mechanisms could be reproduced by increasing the radius of settled spheres (Figure 10(a)). This causes non interconnected pores to appear, while the macropore structure deriving from the largest grain sheltering effect remain to dominate the residual porosity. Here a 15% radius increase has been performed on the plug of Figure 7(n). Another possibility is provided by mapping the spheres according to a given transformation. In Figure 10(b) an example of trigonometric mapping that does not alter the average grain radius is shown, with reference to mixture *D* of Table I.

generate synthetic (but reasonably realistic) granular porous media by simulating the deposition process of spherical grains in the conditions typical of a viscous fluid at rest. Accordingly, the unconsolidated generated medium emerges as the outcome of a physical process, although simplified by neglecting compaction and cementation. The numerical porous media could be used to explore topological properties of the intergranular void space, in correspondence to different grain distribution curves. By solving Equations (2), it will be possible to relate these properties to the hydraulic properties of the flow field at the macroscale.

Although compaction and cementation have not been addressed in this paper, we believe that the generated porous media provide a sound basis to simulate consolidation. A simple example is provided by pressure solution processes, whose dissolution and precipitation effects could be reproduced, as a first approximation, by slightly increasing the radius of deposed spheres, as shown in Figure 10(a). Moreover, we believe that the nucleation and growth of crystals (whose importance for the determination of the hydraulic properties of a rock can hardly be overrated, as shown, for example by Wong *et al.* (1986) and Katz and Thompson (1986)) could be easily implemented by using suitable automata, such as Diffusion Limited Aggregates, (Witten and Sander, 1981; Jullien and Botet, 1987) on a discrete lattice where the generated porous medium has been resampled.

Acknowledgements

This paper benefited from several discussions on micro-scale analysis of creeping flow in porous media. In particular, thanks are due to Dott. Domenico Giordano, *AGIP* modelling department, Prof Giovanni Menduni, Politecnico di Milano, Prof Baldassare Bacchi, Università degli Studi di Brescia, and Prof Paolo Ghilardi, Università di Pavia. Advice by anonymous referees, that contributed to improve the quality of this work, is gratefully acknowledged. This work was supported by funds GNDCI CNR CT 9700007PF42B and MURST 60%.

References

Adler, P. M.: 1992, *Porous Media*, Butterworth, Heinemann, London.
Allen, J. R. L.: 1985, *Principles of Physical Sedimentology*, George Allen & Unwin, London.
Bachmat, Y. and Bear, J.: 1986, Macroscopic modelling of transport phenomena in porous media: 1. The continuum approach, *Transport in Porous Media* **1**, 213–240.
Bear, J.: 1988, *Dynamics of Fluids in Porous Media*, Dover, New York.
Buchalter, B. J. and Bradley, R. M.: 1994, Orientational order in amorphous packings of ellipsoids, *Europhys. Lett*. **26**, 159.
Chen, S., Diemer, K., Doolen, G. D., Eggert, K., Fu, C., Gutman, S. and Travis, B. J.: 1991, Lattice gas automata for flow through porous media, *Physica D* **47**, 72–84.
Coelho, D., Thovert, J.-F. and Adler, P. M.: 1997, Geometrical and transport properties of random packings of spheres and aspherical particles, *Phys. Rev. E* **55**(2), 1959–1978.
Darcy, H. P. G.: 1856, *Les fontaines publiques de la ville de Dijon*, Dalmont, Paris.
DallaGiovanna, S. and Vitali, M.: 1996, *Studio sperimentale sulla valutazione della conduttività idraulica degli ammassi sedimentari incoerenti*, Tesi di Laurea, Politecnico di Milano.
Dexter, A. R. and Tanner, D.W.: 1972, Packing densities of mixtures of spheres with lognormal size distributions, *Nature* **238**, 31–32.
Di Pietro, L. B., Melayah, A. and Zaleski, S.: 1994, Modeling water infiltration in unsaturated porous media by interacting lattice gas cellular automata, *Water Resour. Res.* **30**(10), 2785–2792.
Garde, R. J.: 1972, Bed material characteristics of alluvial streams, *J. Sedim. Geol.* **7**, 2.
Ghilardi, P., Menduni, G. and Rosso, R.: 1991, On the morphogenesis of scaling porous media, *Excerpta* **6**, 207–227.
Ghilardi, P., Kai Kai A. and Menduni, G.: 1993, Self-similar heterogeneity in granular porous media at the representative elementary volume scale, *Water Resour. Res.* **29**(4), 1205–1214.
Gray, W. A.: 1968, *The Packing of Solid Particles*, Chapman & Hall, London.
Haff, P. K., Anderson, R. S.: 1993, Grain scale simulations of loose sedimentary beds: the example of grain-bed impacts in aeolian saltation, *Sedimentology* **40**, 175–198.
Heywood, H.: 1937, Numerical definitions of particle size and shape, *Chemistry and Industry*, 149–154.
Jiang, Z. and Haff, P. K.: 1993, Multiparticle simulation methods applied to the micromechanics of bed load transport, *Water Resour. Res.* **29**(2), 399–412.
Jiang, Z.: 1995, The motion of sediment-water mixtures during intense bedload transport: computer simulations, *Sedimentology* **42**, 935–945.
Jodrey, W. S. and Tory, E. M.: 1985, Computer simulation of close random packing of equal spheres, *Phys. Rev. A* **32**, 2347.
Jullien, R. and Botet, R.: 1987, *Aggregation and Fractal Aggregates*, World Scientific, Singapore.
Jullien, R. and Meakin: 1987, Simple three-dimensional models for ballistic deposition with restructuring, *P. Europhys. Lett.* **4**, 1385.

Katz, A. J. and Thompson, A. H.: 1986, Fractal sandstones pores: implications for conductivity and pore formation, *Phys. Rev. Lett.* **56**(19), 2112.
Kothyari, U. C.: 1995, Frequency distribution of river bed materials, *Sedimentology* **42**, 283–291.
Maier, R. S., Kroll, D. M., Kutsovsky, Y. E., Davis, H. T. and Bernard, R. S.: 1998, Simulation of flow through bead packs using the lattice Boltzmann method, *Phys. Fluids* **10**(1), 60–74.
Martys, N. S., Torquato, S. and Bentz, D. P.: 1994, Universal scaling of fluid permeability for sphere packings, *Phys. Rev. E* **50**(1), 403–408.
Meagher, D. J.: 1980, Octree encoding: a new technique for the representation, manipulation, and display of arbitrary three dimensional objects by computer, Technical Report IPL-TR-80-111, Image Processing Lab., Rensselaer Polytechnic Inst., Troy, N.Y.
Onoda, G. Y. and Liniger, E. G.: 1990, Random loose packings of uniform spheres and the dilatancy onset, *Phys. Rev. Lett.* **64**, 2727.
Pilotti, M. and Menduni, G.: 1997, Application of lattice gas techniques to the study of sediment erosion and transport caused by laminar sheetflow, *Earth Surface Processes and Landforms* **22**, 885–893.
Quintanilla J. and Torquato, S.: 1996, Clustering properties of d-dimensional overlapping spheres, *Phys. Rev. E* **54**, 5331.
Ridgway, K. and Tarbuck, K. J.: 1966, Radial voidage variation in randomly packed beds of spheres of different sizes, *J. Pharm. Pharmacol*. **18** (supplement).
Rothman, D.: 1988, Cellular automaton fluids: a model for flow in porous media, *Geophysics* 53(**4**), 509–518.
Rubinstein, J. and Torquato, S.: 1989, Flow in random porous media: mathematical formulation, variational principles and rigorous bounds, *J. Fluid Mech.* **206**, 25.
Spencer, D. W.: 1963, The interpretation of grain size distribution curves of clastic sediments, *J. Sedim. Petrol.* **33**, 180–190.
Tacher, L., Perrochet, P. and Parriaux, A.:1997, Generation of granular media, *Transport in Porous Media* **26**, 99–107.
Torquato, S.: 1987, Characterization of the microstructure of disordered media: a unified approach, *Phys. Rev. B* **35**, 5385.
Torquato, S. and Lu, B.: 1990, Rigorous bounds on the fluid permeability: effect of polydispersivity in grain size, *Phys. Fluids A* **2**, 487.
Torquato, S.: 1992, Connection between the morphology and effective properties of heterogeneous materials, In: S. Torquato and D. Krajcinovic (eds), *Macroscopic Behavior of Heterogenous Materials from the Microstructure*, American Society of Mechanical Engineers, AMD-Vol. 147, p. 53.
Torquato, S.: 1994, Macroscopic behavior of random media from the microstructure, *Appl. Mech. Rev.* 47.
Turcotte, D. L.: 1986, Fractals and fragmentation, *J. Geophys. Res*. **91**(B2), 1921–1926.
Turcotte, D. L.: 1992, *Fractals and Chaos in Geology and Geophysics*, Cambridge University Press, Cambridge.
Vischer, G. S.: 1969, Grain size distribution and depositional processes, *J. Sedim. Petrol*. **39**, 1074–1106.
Wakeman, R. J.: 1975, Packing densities of particles with lognormal size distributions, *Powder Technol.* **11**, 297–299.
Witten, T. A. and Sander, L. M.: 1981, Diffusion limited aggregation, a kinetic critical phenomenon, *Phys. Rev. Lett.* **47**, 1400–1403.
Wong P. Z., Howard, J. and Lin, J. S.: 1986, Surface roughening and the fractal nature of rocks, Schlumberger-Doll (Research Preprint).
Yerry, M. A. and Shephard, M. S.: 1984, Automatic three-dimensional mesh generation by the modified octree technique, *Int. J. Num. Methods Engng.* **20**, 1965–1990.